THE JOURNAL OF BIOLOGICAL CHEMISTRY VOL. 289, NO. 52, pp. 35724–35730, December 26, 2014

Human NAT10 Is an ATP-dependent RNA Acetyltransferase Responsible for N^4-Acetylcytidine Formation in 18 S Ribosomal RNA (rRNA)*

Received for publication, August 4, 2014, and in revised form, November 11, 2014
Published, JBC Papers in Press, November 19, 2014, DOI 10.1074/jbc.C114.602698

Satoshi Ito[‡], Sayuri Horikawa[‡], Tateki Suzuki[§], Hiroki Kawauchi[§], Yoshikazu Tanaka[§¶], Takeo Suzuki[‡], and Tsutomu Suzuki[‡1]

From the [‡]Department of Chemistry and Biotechnology, Graduate School of Engineering, The University of Tokyo, 7-3-1 Hongo, Bunkyo-ku, Tokyo 113-8656 and the [§]Graduate School of Life Science and [¶]Faculty of Advanced Life Science, Hokkaido University, Sapporo 060-0810, Japan

Background: Post-transcriptional modifications of rRNAs play important roles in biogenesis and function of ribosome.
Results: NAT10 is an ATP-dependent RNA acetyltransferase responsible for N^4-acetylcytidine formation of 18 S rRNA.
Conclusion: NAT10 and ac^{4}C1842 are required for pre-18 S rRNA processing.
Significance: 40 S subunit formation is regulated by a single acetylation of 18 S rRNA, implying a regulatory mechanism for ribosome biogenesis by sensing the cellular energy budget.

Human *N*-acetyltransferase 10 (NAT10) is known to be a lysine acetyltransferase that targets microtubules and histones and plays an important role in cell division. NAT10 is highly expressed in malignant tumors, and is also a promising target for therapies against laminopathies and premature aging. Here we report that NAT10 is an ATP-dependent RNA acetyltransferase responsible for formation of N^4-acetylcytidine (ac^{4}C) at position 1842 in the terminal helix of mammalian 18 S rRNA. RNAi-mediated knockdown of NAT10 resulted in growth retardation of human cells, and this was accompanied by high-level accumulation of the 30 S precursor of 18 S rRNA, suggesting that ac^{4}C1842 formation catalyzed by NAT10 is involved in rRNA processing and ribosome biogenesis.

The ribosome is a large ribonucleoprotein complex that translates the genetic information carried by mRNA into protein sequence. The eukaryotic ribosome consists of the small 40 S subunit and the large 60 S subunit, each of which contains rRNAs and ribosomal proteins. In mammals, 47 S pre-rRNAs transcribed from the rDNA repeat region are processed into 18 S (see Fig. 1*A*), 5.8 S, and 28 S rRNAs through multistep processing events (see Fig. 2*E*) (1). More than 200 factors and small nucleolar RNAs are involved in ribosome assembly, and mutations in these assembly factors often result in pathological consequence (2, 3). During rRNA processing, rRNAs are modified post-transcriptionally; these modifications are involved in fine-tuning translational fidelity and/or modulating ribosome biogenesis (4). The most abundant rRNA modifications in mammals, 2′-*O*-methylation and pseudouridylation (Ψ), are introduced by box C/D and box H/ACA small nucleolar RNA-guided enzymes, respectively (5). In addition, 18 S and 28 S rRNAs contain several small nucleolar ribonucleoprotein-independent modifications (4), which are introduced by specific RNA-modifying enzymes. N^4-Acetylcytidine (ac^{4}C)[2] (see Fig. 1*A*) is present in 18 S rRNA from rat, chicken, and *Saccharomyces cerevisiae*, although the exact positions of ac^{4}C in these species remained unknown (6). In *Dictyostelium discoideum*, ac^{4}C is present at position 1844 in the 3′ terminal region of 18 S rRNA (7). Together, these observations indicate that ac^{4}C is a highly conserved modification in eukaryotic 18 S rRNAs.

Very recently, we reported that ac^{4}C is present at position 1773 in the 18 S rRNA of *S. cerevisiae* and found an essential gene, *KRE33*, which we renamed *RRA1* (ribosomal RNA cytidine acetyltransferase 1) encoding an RNA acetyltransferase responsible for ac^{4}C1773 formation (8). Here, we report that NAT10, a human homolog of Rra1p, is an ATP-dependent RNA acetyltransferase responsible for formation of ac^{4}C at position 1842 in mammalian 18 S rRNA.

EXPERIMENTAL PROCEDURES

Cell Lines and Growth Conditions—HeLa and HEK293 cells were grown in DMEM supplemented with 10% FBS, at 37 °C under a humidified atmosphere containing 5% CO_2.

RNA Extraction and Preparation of 18 S rRNA—Total RNA was extracted from cells using TriPure isolation reagent (Roche Diagnostics) and resolved by PAGE on 4% polyacrylamide gels containing 7 M urea. 18 S rRNA was excised from the gel and extracted from the gel slice by the "crush and soak" method in elution buffer (0.3 M NaOAc, 1 mM EDTA, 0.1% SDS).

RNA Mass Spectrometry—Highly sensitive analysis of RNA fragments by mass spectrometry was carried out essentially as described previously (9, 10). The isolated 18 S rRNA was digested with RNase T_1 at 37 °C for 30 min in a 10-μl reaction mixture containing 10 mM ammonium acetate (pH 5.3) and 5 units/μl RNase T_1 (Epicentre), followed by the addition of an equal volume of 0.1 M triethylamine acetate (pH 7.0). The digest was then subjected to capillary LC coupled with nano-electrospray ionization-mass spectrometry (ESI-MS) using a linear ion trap-orbitrap hybrid mass spectrometer (LTQ Orbitrap XL, Thermo Fisher Scientific).

* This work was supported by grants-in-aid for scientific research on priority areas from the Ministry of Education, Science, Sports, and Culture of Japan (to Tsutomu Suzuki).
[1] To whom correspondence should be addressed. E-mail: ts@chembio.t.u-tokyo.ac.jp.

[2] The abbreviations used are: ac^{4}C, N^4-acetylcytidine; NAT10, *N*-acetyltransferase 10; CID, collision-induced dissociation; ESI, electrospray ionization; DIG, digoxigenin; ITS1, internal transcribed spacer 1; ETS, external transcribed spacer.

TABLE 1
List of primers, probes, and siRNAs used in this study
Fw, forward; Rv, reverse.

Purpose	Direction	Name	5′ to 3′ sequence
PCR primers			
DIG probe ETS1 (A0 to 1) of human	Fw	DIG-human ETS1 (A0 to 1)-F	TAATACGACTCACTATAGGGCTGTCCGGCAGGGACCAC
	Rv	DIG-human ETS1 (A0 to 1)-R	CCCGTGGTCTCTCGTCTTCT
DIG probe ITS1 (E to C) of human	Fw	DIG-human ITS1(EtoC)-F	TAATACGACTCACTATAGGGGAGGAGGGCACCGAGACC
	Rv	DIG-human ITS1(EtoC)-R	GCGAGAGCCGGAGAACTC
DIG probe ETS1 (C to 2) of human	Fw	DIG-human ITS1 (Cto2)-F	TAATACGACTCACTATAGGGGTCGGAAGGTTTCACACCAC
	Rv	DIG-human ITS1 (Cto2)-R	GTCGGGTGGGGGCTTTAC
T7 transcription for a substrate RNA	Fw	Substrate-F	GCTAATACGACTCACTATAGTAAAAGTCGTAACAAGGTTTCCGTA
	Rv	Substrate-R	TAATGATCCTTCCGCAGGTTCACCTACGGAAACCTTGTTACGAC
Recombinant Nat10 expression	Fw	Nat10-SbfI-F	TGCGCCTGCAGGGGAATCGGAAGAAGGTGGATAACCG
	Rv	Nat10-AscI-R	ATTGGCGCGCCCTACTTCTTTCGCTTCAGTTTCATATCC
Checking for RNAi knockdown by quantitative RT-PCR	Fw	NAT10_fw	GGACCTGCCTCCTTTACTCC
	Rv	NAT10_rv	CTTCAGCATGATGCACGAGT
	Fw	ACTB_fw	GGACTTCGAGCAAGAGATGG
	Rv	ACTB_rv	AGCACTGTGTTGGCGTACAG
siRNA			
Negative control	Sense	siLUC	CGUACGCGGAAUACUUCGAAG
	Antisense	siLUC	UCGAAGUAUUCCGCGUACGAU
Knockdown of NAT10	Sense	siNAT10a	GCAAGAAGUUGAAGAACAGAG
	Antisense	siNAT10a	CUGUUCUUCAACUUCUUGCAU
	Sense	siNAT10b	CGGCCUUCAGUGCUGUGGUGUUAUAAG
	Antisense	siNAT10b	UAUAACACCACAGCACUGAAGGCCGAU
	Sense	siNAT10c	AGGAGAAACACAAGAAGGAAG
	Antisense	siNAT10c	UCCUUCUUGUGUUUCUCCUAU

RNAi—Sequences of siRNAs used in this study are listed in Table 1. Two siRNAs targeting NAT10, siNAT10a and siNAT10c, were designed using the "siExplorer" algorithm (11). The sequence of siNAT10b was obtained from the literature (12). These siRNAs were chemically synthesized by FASMAC Co., Ltd. HeLa cells (2.5×10^5 cells) or HEK293 cells (2.5×10^5 cells) were transfected with siRNA (1 or 10 nM, respectively) using Lipofectamine RNAiMAX (Invitrogen). Cells were harvested 4 days after transfection. The efficiency of RNAi was estimated by measuring the steady-state level of *NAT10* mRNA, normalized to the level of *ACTB* mRNA, on a LightCycler 480 real-time PCR system (Roche Diagnostics). Primer sets are listed in Table 1. Knockdown of NAT10 was confirmed by Western blotting using anti-NAT10 antibody (Clone B-4, Santa Cruz Biotechnology Inc.).

Measuring Cell Proliferation—HeLa cells (2.5×10^5 cells) were transfected with siRNA (final concentration 1 nM) as described above. Cell proliferation in each well was evaluated daily using alamarBlue (BIOSOURCE International, Inc.) according to the manufacturer's instructions. The absorbance of the wells was read at 570 nm and 600 nm with a SpectraMax 190 plate reader (Molecular Devices, Inc.). Cell proliferation was calculated from fraction of the reduced dye as percentage of reduced.

Flow Cytometry—HeLa cells were harvested 4 days after siRNA transfection, stained with annexin V and propidium iodide using the annexin V-FITC apoptosis kit (BioVision), and analyzed by flow cytometry (FACS, BD Biosciences).

Northern Blotting—Total RNA (1 μg) in loading solution (10 mM MOPS, 2.5 mM NaOAc (pH 5.0), 0.5 mM EDTA-NaOH (pH 8.0), 6.5% formaldehyde, and 50% deionized formamide) was denatured at 65 °C for 10 min and left on ice. After the addition of 2 μl of dye solution (0.25% bromphenol blue, 0.25% xylene cyanol, 50% glycerol, and 1 mM EDTA-NaOH (pH 8.0)), total RNA was electrophoresed on a 1% agarose gel (10 × 10 cm, SeaKem GTG agarose, TaKaRa) containing 0.6 M formaldehyde in MOPS buffer (20 mM MOPS, 5 mM NaOAc (pH 5.0), 1 mM EDTA-NaOH (pH 8.0)) for 2.5 h at 100 V. The gel was stained with ethidium bromide in alkaline solution (50 mM NaOH and 1 μg/ml ethidium bromide), followed by two rounds of neutralization with 200 mM NaOAc (pH 5.0) for 20 min each. rRNAs in the gel were visualized using a FLA7000 imaging analyzer (Fujifilm). After equilibrating the gel twice with 10 × SSC for 10 min each, RNAs were transferred to a Hybond-N^+ nylon membrane (GE healthcare) in 10 × SSC using a model 785 vacuum blotter (Bio-Rad).

Northern blotting was carried out using the DIG Northern starter kit (Roche Diagnostics). The RNA probes (~200-mers, complementary to 5′-ETS or ITS1) were transcribed by T7 RNA polymerase in the presence of digoxigenin-11-UTP. Primer sequences used to amplify the templates for the RNA probes are listed in Table 1. Hybridization was carried out at 68 °C overnight. The hybridized bands were visualized by CDP-Star chemiluminescence (Roche Diagnostics), using alkaline phosphatase-conjugated anti-digoxigenin, and detected on an LAS 4000 mini (GE healthcare).

Sucrose Density Gradient Centrifugation and Ribosomal Subunit Profiling—HeLa cells ($1.6–2.4 \times 10^6$ cells) were treated with siRNAs for luciferase (siLUC) and NAT10 (siNAT10c) as described under "RNAi." The cells were harvested, washed with ice-cold PBS, and resuspended with 300 μl of lysis buffer (20 mM Tris-HCl (pH 7.4), 200 mM NaCl, 15 mM EDTA, 0.5% Triton X-100 (v/v), 1× cOmplete EDTA-free protease inhibitor mixture (Roche Diagnostics), 0.2 units/μl SUPERase•In RNase inhibitor (Life Technologies)), followed by passing a 25-gauge needle 20 times to prepare the whole-cell lysate. The lysate was gently rotated for 10 min at 4 °C and centrifuged at 10,000 × *g* for 10 min at 4 °C. The supernatant was transferred to a new tube, recentrifuged at 10,000 × *g* for 10 min at 4 °C, and loaded onto a 10–40% (w/v) linear gradient of sucrose containing 20 mM Tris-HCl (pH 7.4), 200 mM NaCl, 15 mM EDTA, 1 mM DTT, followed by ultracentrifugation in SW41Ti rotor (Beckman

Coulter) at 37,000 rpm for 3.5 h at 4 °C. The sucrose gradient was fractionated by a Piston gradient fractionator (BioComp), and ribosomal subunits were monitored by absorbance at 254 nm using a UV monitor (AC-5200, ATTO) and a digital recorder (AC-5150, ATTO).

Expression and Purification of Recombinant Nat10—The gene of mouse *Nat10* was amplified by PCR using a cDNA clone from the Mammalian Gene Collection (Invitrogen) as a template, KOD-Plus-DNA polymerase (Toyobo), and a set of primers (Table 1). The PCR product was inserted into the SbfI and AscI sites of a modified pPICZ vector (Invitrogen) to generate pPICZ-Nat10. The resultant vector was linearized with BstXI and then electroporated into *Pichia pastoris* strain SMD1168H. Electroporation was performed in a 0.2-cm cuvette in a Micro-Pulser (Bio-Rad) with a pulse voltage of 2 kV. Overproducing transformants harboring multiple copies of the *Nat10* genes were selected with 500 μg/ml Zeocin on YPD plates and then cultured in buffered glycerol-complex (BMGY) medium at 30 °C for 24 h. Cells were collected by centrifugation at 4,500 × *g* for 15 min and then disrupted using a Multi-Beads Shocker (Yasui Kikai) in disruption buffer consisting of 50 mM Tris-HCl (pH 8.0), 500 mM NaCl, 10% glycerol, 0.1% Triton X-100, 1 mM PMSF, and 5 mM 2-mercaptoethanol. Cell debris was removed by centrifugation at 40,000 × *g* for 30 min at 10 °C, and the supernatant was loaded onto a HisTrap HP column (GE Healthcare) pre-equilibrated with His binding buffer consisting of 20 mM HEPES-NaOH (pH 7.6), 400 mM NaCl, 10% glycerol, and 5 mM 2-mercaptoethanol. After washing with His binding buffer containing 40 mM imidazole and 0.05% cOmplete EDTA-free protease inhibitor cocktail tablets (Roche Diagnostics), recombinant Nat10 with N-terminal hexahistidine tag was eluted with a 0.04–0.4 M gradient of imidazole in His binding buffer. Fractions containing Nat10 were loaded onto a HiTrap Heparin HP column (GE Healthcare) pre-equilibrated with heparin binding buffer consisting of 20 mM HEPES-NaOH (pH 7.6), 300 mM NaCl, 10% glycerol, and 5 mM 2-mercaptoethanol. The recombinant Nat10 was eluted with a 0.3–2 M gradient of NaCl in heparin binding buffer. The collected fractions were further purified on a HiLoad 26/60 Superdex 200 column (GE Healthcare) pre-equilibrated with size exclusion chromatography (SEC) buffer consisting of 20 mM HEPES-NaOH (pH 7.6), 300 mM NaCl, 10% glycerol, and 1 mM dithiothreitol. The purified Nat10 was stored at −80 °C until use.

In Vitro Reconstitution of ac^{4}C1842 Formation—The DNA templates for *in vitro* transcription of RNA fragments carrying helix 45 of 18 S rRNA and its variants were constructed by PCR using synthetic DNAs (Table 1). The substrate RNA was transcribed by T7 RNA polymerase essentially as described (13). The transcripts were extracted from the reaction mixture with phenol-chloroform, passed through a NAP-5 column (GE healthcare) to remove free NTPs, and precipitated with ethanol. The transcript was further purified on a 10% PAGE gel containing 7 M urea.

In vitro reconstitution of ac^{4}C formation was carried out at 30 °C for 2 h in a reaction mixture (10 μl) consisting of 50 mM HEPES-KOH (pH 7.6), 150 mM KCl, 5 mM $MgCl_2$, 1 mM DTT, 1 mM ATP, 1 mM acetyl-CoA, 1 μM substrate RNA, and 5.1 μM recombinant Nat10. After the reaction, the RNA fragment was extracted with phenol-chloroform, followed by ethanol precipitation. The ac^{4}C formation was analyzed by mass spectrometry as described above.

RESULTS AND DISCUSSION

To determine the exact position of ac^{4}C modification, we performed mass spectrometric analysis on 18 S rRNA from HEK293 cells. RNase T_1-digested RNA fragments of 18 S rRNA were subjected to capillary LC coupled with nano-ESI-MS to detect RNA fragments containing modified nucleotides. We were able to assign most RNA fragments deduced from the human 18 S rRNA sequence with modified nucleotides. The doubly charged negative ion of the ac^{4}C-containing hexamer was detected (Fig. 1*B*) and further analyzed by collision-induced dissociation (CID). This analysis revealed that the hexamer sequence was UUUCac^{4}CGp (Fig. 1*C*); thus, ac^{4}C is present at position 1842 of the helix 45 in 18 S rRNA (Fig. 1*A*), which is equivalent to ac^{4}C1844 in *D. discoideum* 18 S rRNA (7) and ac^{4}C1773 in *S. cerevisiae* 18 S rRNA (8).

ac^{4}C is a modified base frequently found in tRNAs and rRNA from all domains of life (14). In bacteria, ac^{4}C is present at the wobble position of elongator $tRNA^{Met}$. We previously identified $tRNA^{Met}$ cytidine acetyltransferase (TmcA) in *Escherichia coli*, which catalyzes ac^{4}C formation in the presence of acetyl-CoA and ATP (15). TmcA has two catalytic domains, RNA helicase (ATPase) and *N*-acetyltransferase. According to the crystal structure of *E. coli* TmcA (16), the RNA helicase domain contains ADP (a hydrolysis product of ATP), whereas the *N*-acetyltransferase domain interacts with acetyl-CoA. Biochemical and genetic studies of *E. coli* TmcA revealed that both domains are required for ac^{4}C formation in tRNA (15, 16). Orthologs of *tmcA* are widely distributed among archaea and eukaryotes. Based on the fact that ac^{4}C is present in the 3′-terminal region of 18 S rRNAs in eukaryotes (6, 7), the eukaryotic homolog of TmcA was proposed to be the RNA acetyltransferase responsible for ac^{4}C formation in 18 S rRNA (15). In fact, we recently reported that Rra1p (ribosomal RNA cytidine acetyltransferase 1), which is a yeast homolog of TmcA, catalyzes ac^{4}C1773 formation using acetyl-CoA and ATP as substrates (8).

In humans and mouse, *N*-acetyltransferase 10 (NAT10 and Nat10, respectively) is an ortholog of bacterial TmcA and yeast Rra1p. Human NAT10 (also known as hALP) was initially identified as a transcriptional factor that interacts with the promoter region of hTERT (human telomerase reverse transcriptase) (17). Recombinant NAT10 (amino acids 164–834) lacking the N-terminal domain has the ability to acetylate calf thymus histones *in vitro* in the presence of acetyl-CoA (without ATP), indicating that NAT10 has a histone acetyltransferase activity that might promote hTERT transcription via decondensation of chromatin structure (17). In addition, it was reported that NAT10 is associated with U3 small nucleolar RNA, and acetylates upstream binding factor to activate rRNA transcription (18). NAT10 is predominantly localized to the nucleolus during interphase, but to the mitotic midbody during telophase (19). Depletion of NAT10 causes defects in nucleolar assembly and cytokinesis, and also reduces the level of acetylated α-tubulin, leading to G_2/M arrest (19). NAT10 can also

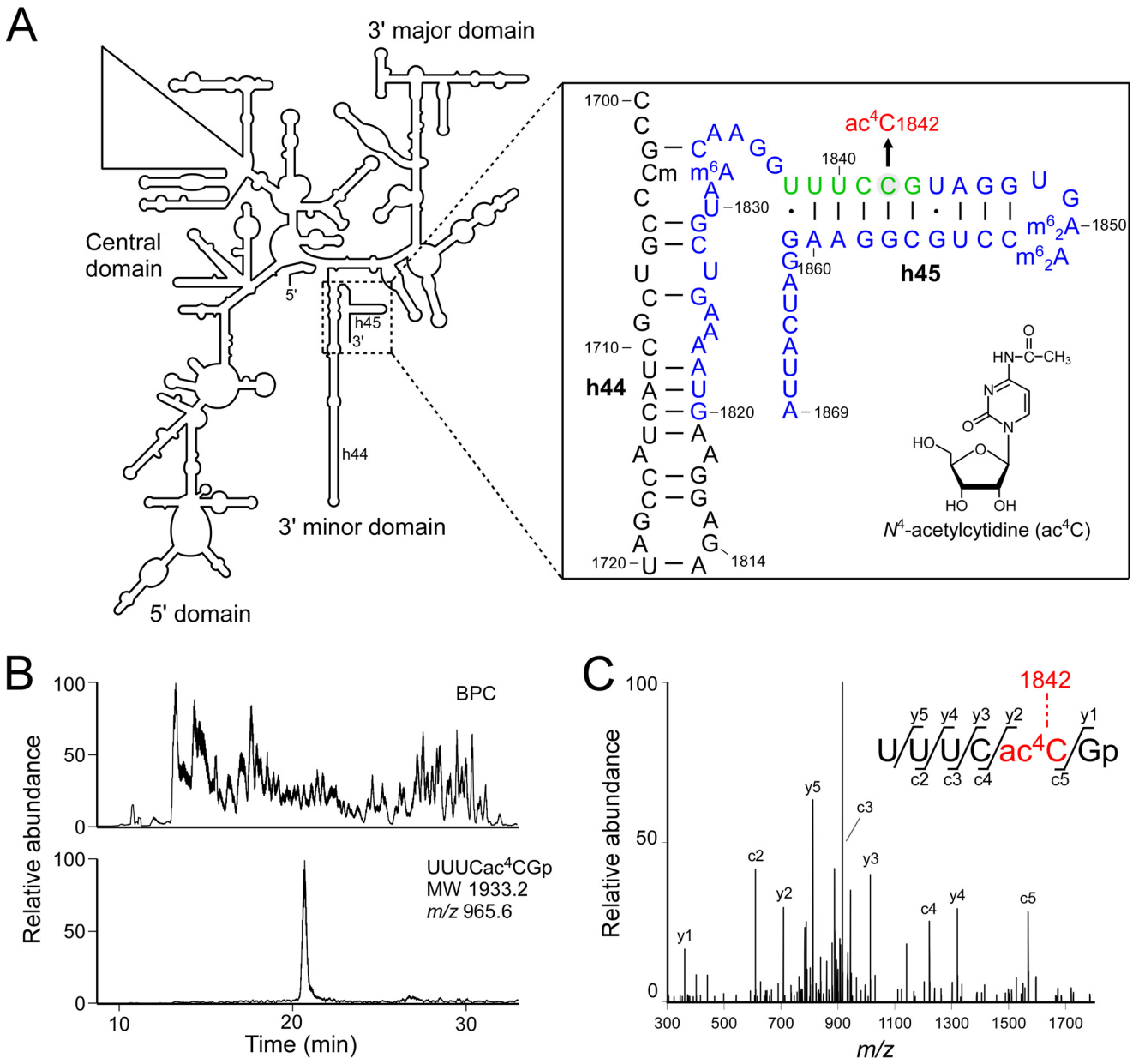

FIGURE 1. ***N*^{4}-Acetylcytidine is present at position 1842 in human 18 S rRNA.** *A*, the secondary structure of human 18 S rRNA (*left*) with a detailed description of helix 45 and the surrounding region (*right box*), with modified nucleosides: ac^{4}C at position 1842, N^6,N^6-dimethyladenosine ($m^6{}_2A$) at positions 1850 and 1851, 2′-*O*-methylcytidine (*Cm*) at position 1703, and N^6-methyladenosine (m^6A) at position 1832. The *in vitro* transcribed RNA segment (G1820–A1869) used for ac^{4}C formation is shown in *blue*. The ac^{4}C-containing hexamer fragment generated by RNase T_1 digestion is shown in *green*. Watson-Crick base pairs and wobble pairs are shown as *bars* and *dots*, respectively. *B*, capillary LC/ESI-MS analysis of fragments of RNase T_1-digested 18 S rRNA from HEK293 cells. The *upper panel* shows the base-peak chromatogram (*BPC*), and the *lower panel* shows the mass chromatogram of the doubly charged ion of the ac^{4}C-containing hexamer fragment (UUUCac^{4}CGp, *m/z* 965.6). *C*, CID spectrum of the ac^{4}C-containing hexamer fragment. The doubly charged ion (*m/z* 965.6) was used as the parent for CID. The sequence was confirmed by assignment of the product ions. The nomenclature for product ions is according to a previous study (24).

acetylate porcine tubulin *in vitro* (20), although the acetylated residues have not yet been determined. These observations indicate that NAT10 plays an important role in cell division by facilitating reformation of the nucleolus and midbody in the late phase of mitosis.

To determine whether NAT10 is the RNA acetyltransferase responsible for ac^{4}C formation in 18 S rRNA, we knocked down NAT10 in HeLa cells using three distinct siRNAs. We confirmed the absence of endogenous NAT10 in knockdown cells by Western blotting (Fig. 2*A*). As reported previously (19), NAT10 knockdown cells grew more slowly than control cells (siLUC) (Fig. 2*B*). Four days after the transfection, the NAT10 knockdown cells were harvested and stained with annexin V and propidium iodide, followed by flow cytometry. The fraction of apoptotic cells increased significantly upon NAT10 depletion (Fig. 2*C*), suggesting that the growth retardation of NAT10 knockdown cells can be partly explained by an elevated rate of apoptotic death. Next, we prepared 18 S rRNA from the knockdown cells and subjected it to capillary LC/ESI-MS analysis. Intriguingly, the level of the ac^{4}C1842-containing hexamer (UUUCac^{4}CGp) was markedly reduced relative to the control fragment in NAT10 knockdown cells (Fig. 2*D*). This result

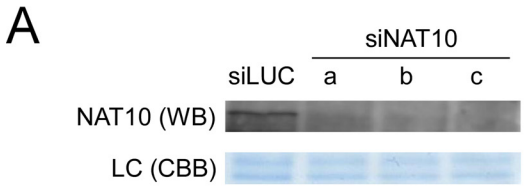
A
siNAT10
siLUC
a
b
c
NAT10 (WB)
LC (CBB)

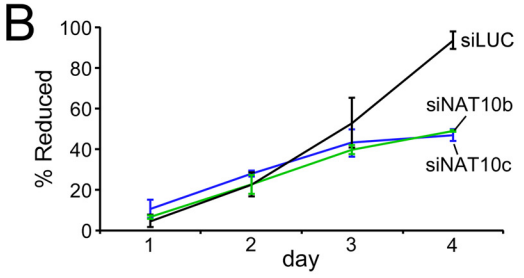
B
% Reduced
day
siLUC
siNAT10b
siNAT10c

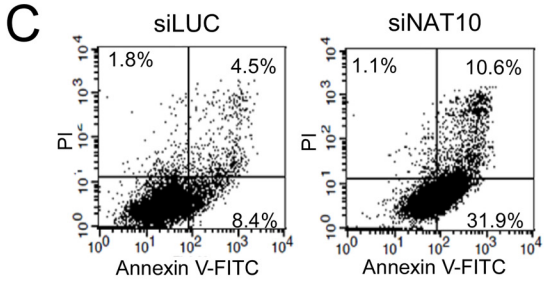
C
siLUC
siNAT10
1.8%
4.5%
8.4%
1.1%
10.6%
31.9%
PI
Annexin V-FITC

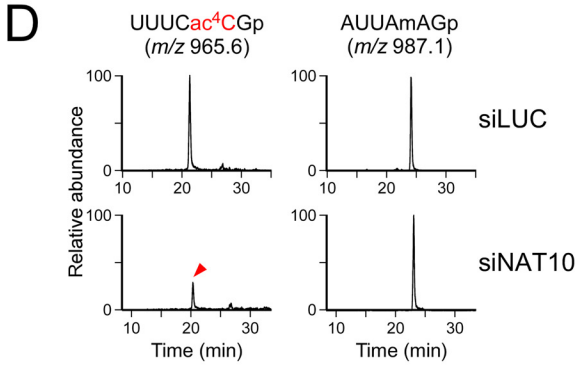
D
UUUCac4CGp
(m/z 965.6)
AUUAmAGp
(m/z 987.1)
siLUC
siNAT10
Relative abundance
Time (min)

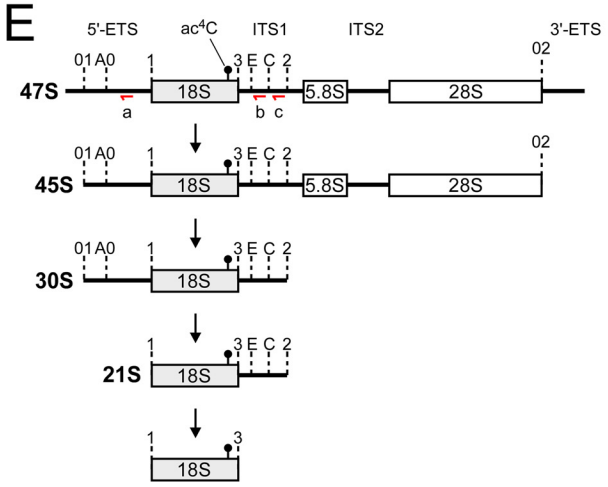
E
5'-ETS
ac4C
ITS1
ITS2
3'-ETS
47S
45S
30S
21S
18S
5.8S
28S

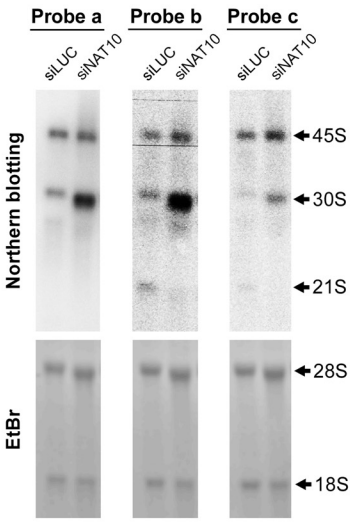
F
Probe a
Probe b
Probe c
siLUC
siNAT10
Northern blotting
EtBr
45S
30S
21S
28S
18S

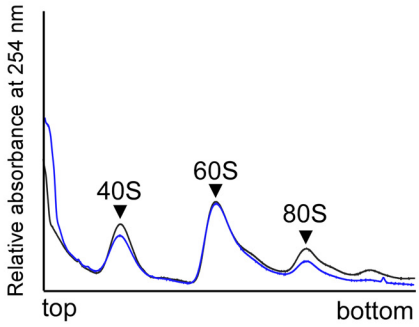
G
Relative absorbance at 254 nm
40S
60S
80S
top
bottom

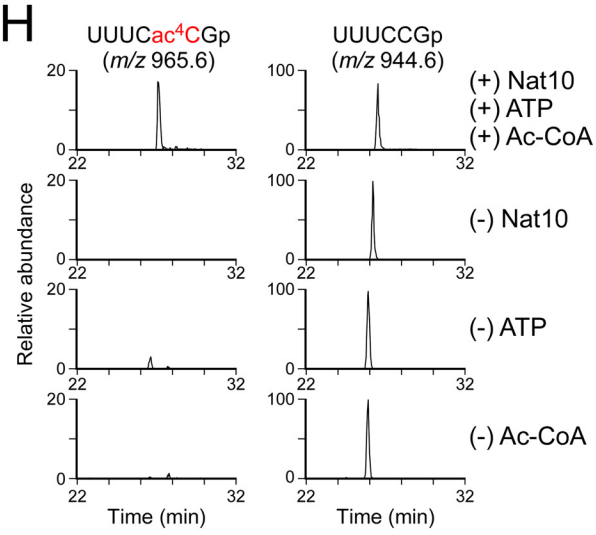
H
UUUCac4CGp
(m/z 965.6)
UUUCCGp
(m/z 944.6)
(+) Nat10
(+) ATP
(+) Ac-CoA
(-) Nat10
(-) ATP
(-) Ac-CoA
Relative abundance
Time (min)

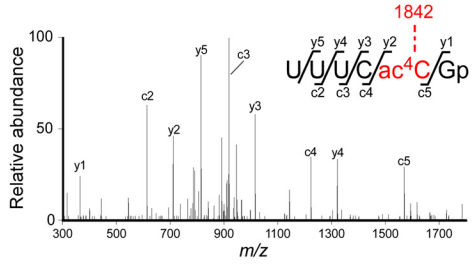
I
1842
U/U/U/C/ac4C/Gp
Relative abundance
m/z

strongly suggested that NAT10 is responsible for ac^{4}C1842 formation in 18 S rRNA. In the case of *S. cerevisiae*, *RRA1* is an essential gene, and temporal depletion of Rra1p resulted in significant accumulation of the 23 S pre-rRNA, leading to complete loss of 18 S rRNA and 40 S subunit (8). We observed complete absence of ac^{4}C1773 in the accumulated 23 S pre-rRNA, but little reduction of ac^{4}C1773 in 18 S rRNA, which is likely to originate from a residual pool of 40 S subunit that accumulated in the cytoplasm before depletion of Rra1p (8). These results suggest that ac^{4}C1773 formation catalyzed by Rra1p plays an essential role in processing of the 23 S pre-rRNA to yield 18 S rRNA. Unlike the case of *S. cerevisiae*, apparent reduction of ac^{4}C1842 in 18 S rRNA was observed in human cells upon NAT10 depletion. The ac^{4}C1842 formation mediated by NAT10 is not essential for pre-rRNA processing to yield 18 S rRNA.

Given that NAT10 localizes to the nucleolus and is involved in nucleolar assembly (19), it is likely that this protein plays a role in ribosome biogenesis. To examine whether 18 S rRNA processing is affected by NAT10 knockdown, we detected precursors of 18 S rRNAs by Northern blotting with three probes complementary to the 5′-ETS and ITS1 (Fig. 2*E*). Processing of the 47 S pre-rRNA was initiated with endonucleolytic cleavages at site 01 in the 5′-ETS and site 02 in the 3′-ETS to generate 45 S pre-rRNA, which was then processed into 30 S pre-rRNA by cleavage at site 2 in ITS1, splitting pathways for small subunit and large subunit maturation. 30 S pre-rRNA was further processed into 21 S pre-rRNA by removal of the 5′-ETS. The 45 S and 30 S pre-rRNAs were detected by the three probes, whereas 21 S pre-rRNA was detected by two probes (b and c) complementary to ITS1 (Fig. 2*F*). Upon NAT10 knockdown, 30 S pre-rRNA clearly accumulated (Fig. 2*F*), concomitant with a reduction in the level of 21 S pre-rRNA (Fig. 2*F*). These results indicate that ac^{4}C1842 formation mediated by NAT10, or the enzymatic activity of NAT10 in the pre-ribosomal particle, is required to process site 1 of 30 S pre-rRNA to yield 21 S pre-rRNA. In fact, the steady-state level of 18 S rRNA was reduced upon NAT10 knockdown, relative to the control cell treated with siLUC, whereas the 28 S rRNA was unaffected (Fig. 2*F*). The 18 S/28 S ratio of the NAT10 knockdown cell was reduced to 82 ± 4% that of the control cell (Fig. 2*F*), indicating that NAT10 is involved in biogenesis of 18 S rRNA. Then, we compared the steady-state level of ribosomal subunits between the NAT10 knockdown cell and the control cell by sucrose density gradient centrifugation analysis (Fig. 2*G*). The level of 40 S subunit was apparently reduced in NAT10 knockdown cell, whereas 60 S subunit was unchanged. The 40 S/60 S ratio of the NAT10 knockdown cell was reduced to 77% that of the control cell. The residual 80 S ribosome was also reduced in the NAT10 knockdown cell, indicating a shortage of 40 S subunit relative to 60 S subunit.

Several underlying mechanisms are possible. RNA helicase activity of NAT10 might modulate the small subunit processome to facilitate the rRNA processing; alternatively, a putative reader protein that specifically recognizes ac^{4}C1842 might recruit an unidentified endonuclease responsible for this site. Further study will be necessary to reveal in molecular detail why this single acetylation mediated by NAT10 is involved in rRNA processing.

To detect an appropriate enzymatic activity of NAT10 to participate in ac^{4}C formation, we obtained recombinant Nat10 expressed in *P. pastoris* and purified it to homogeneity. A 50-mer RNA segment including helix 45 (G1820–A1869) (Fig. 1*A*) was transcribed *in vitro* and used as the substrate for ac^{4}C formation by recombinant Nat10. After the reaction, the RNA segment was digested with RNaseT_1 and subjected to LC/ESI-MS to detect the ac^{4}C-modified fragment. As shown in Fig. 2*H*, the ac^{4}C-containing hexamer was clearly detected only in the presence of both ATP and acetyl-CoA. CID analysis revealed that the ac^{4}C in the hexamer was in position 1842 (Fig. 2*I*).

A truncated recombinant NAT10 (amino acids 164–834) lacking the N-terminal RNA helicase domain has *in vitro* lysine acetyltransferase activity toward histones in the presence of acetyl-CoA; this activity does not require ATP (17). In this study, we clearly showed that a full-length Nat10 has RNA acetyltransferase ability that can catalyze formation of ac^{4}C1842 in 18 S rRNA in the presence of both acetyl-CoA and ATP; thus,

FIGURE 2. **NAT10 is an ATP-dependent RNA acetyltransferase involved in 18 S rRNA processing.** *A*, Western blotting (*WB*) of endogenous NAT10 to estimate the knockdown efficiency of three siRNAs against NAT10 (siNAT10) and an siRNA against luciferase (siLUC), used as a negative control. Coomassie Brilliant Blue (*CBB*) staining of each sample is shown as a loading control (*LC*). Knockdown efficiencies of the three siRNAs, estimated from the levels of *NAT10* mRNA (normalized by *ACTB* mRNA), were 10.6% (siNAT10a), 12.5% (siNAT10b), and 3.2% (siNAT10c), respectively. *B*, growth curves of HeLa cells treated with siRNAs against NAT10 (*green* and *blue lines* for siNAT10b and siNAT10c, respectively) or luciferase (*black line* for siLUC). Each plot is the average of three independent cultures (bars, ±S.D.). *C*, flow cytometry of HeLa cells treated with siRNAs against NAT10 (*right panel*) or luciferase (*left panel*), stained with annexin V-FITC (*x*-axis) and propidium iodide (*y*-axis). *D*, capillary LC/ESI-MS analyses of fragments of RNase T_1-digested 18 S rRNAs from the HEK293 cells treated with siNAT10a against NAT10 (*lower panels*) or luciferase (*upper panels*). Mass chromatograms of the doubly charged ions of the ac^{4}C-containing hexamers (UUUCac^{4}CGp, *m/z* 965.6) and control fragments (AUUAmAGp, *m/z* 987.1) are shown in the *left* and *right panels*, respectively. The intensities of the ac^{4}C-containing hexamers in the mass chromatograms were normalized to those of the control fragments. *E*, schematic depiction of the rRNA processing pathways in humans. In the canonical pathway, 47 S pre-rRNA is processed by endonucleolytic cleavages at sites 01 and 02 to yield 45 S pre-rRNA, which is then processed into 30 S pre-rRNA by cleavage at site 2 in ITS1. Precursors for large subunit formation are not shown. 30 S pre-rRNA is further processed into 21 S pre-rRNA by removal of the 5′-ETS. Finally, 18 S rRNA is produced by removal of ITS1. Complementary regions of probes a, b, and c are indicated. The position of ac^{4}C1842 is indicated by the *circle flag*. Processing sites in pre-rRNA are indicated. *F*, accumulation of 30 S pre-rRNA and disappearance of 21 S pre-rRNA upon NAT10 depletion by siNAT10b. Precursors of 18 S rRNA were detected by Northern blotting. Steady-state levels of 28 S and 18 S rRNAs were visualized by EtBr staining, as a loading control. The 45 S and 30 S pre-rRNAs were detected by all three probes, whereas 21 S pre-rRNA was detected only by probes b and c. *G*, sucrose density gradient centrifugation profiling of ribosomal subunits in HeLa cells treated with siRNAs for luciferase (siLUC, *black line*) and NAT10 (siNAT10c, *blue line*). Absorbance at 254 nm was monitored from the top to bottom of the centrifugation tubes. *H*, *in vitro* reconstitution of ac^{4}C1842 in the 50-mer RNA segment, including helix 45 (Fig. 1*A*) in the presence or absence of recombinant Nat10, ATP, and acetyl-CoA. The *left* and *right panels* show mass chromatograms of the hexamer fragments carrying ac^{4}C1842 (UUUCac^{4}CGp, *m/z* 965.6) and C1842 (UUUCCGp, *m/z* 944.6), respectively. *I*, confirmation of the reconstituted ac^{4}C1842 in the 50-mer RNA fragment. A CID spectrum of the ac^{4}C-containing hexamer fragment digested with RNase T_1 is shown. The doubly charged ion (*m/z* 965.6) was used as the parent for CID. The sequence was confirmed by assignment of the product ions. Nomenclature for product ions is as suggested in a previous study (24).

ac^4C1842 formation requires both catalytic domains of NAT10. It remains to be determined whether full-length NAT10 has efficient and specific lysine acetyltransferase activity toward histones or other proteins.

Collectively, the results of this and previous studies indicate that NAT10 has multiple functions required for ribosome biogenesis, nucleolar architecture, cytokinesis, and mitosis. Moreover, NAT10 is highly expressed in malignant tumors (19, 21), and it is essential for growth of a subtype of epithelial ovarian cancer with poor prognosis (22). Recent work demonstrated that NAT10 is the molecular target of a chemical compound called "Remodelin," which treats laminopathies, including premature aging syndromes, by correcting nuclear architecture (20). Functional studies of NAT10 as an rRNA acetyltransferase should facilitate development of novel strategies for treating cancer and premature aging.

Identification of NAT10 as a rRNA acetyltransferase provides a conceptual advance in RNA epigenetics (23). In *S. cerevisiae*, upon depletion of nuclear acetyl-CoA, we observed temporal accumulation of the 23 S pre-rRNA, indicating that Rra1p modulates 40 S biogenesis by sensing nuclear acetyl-CoA concentration (8). Further studies will be required in mammals to investigate the physiological significance of ac^4C modification of 18 S rRNA in coordination with ribosome biogenesis with the cellular energy budget.

Acknowledgments—We are grateful to the members of the Suzuki laboratory, in particular, Yuriko Sakaguchi, Satoshi Kimura, and Yoshiho Ikeuchi, for technical support and many insightful discussions. Special thanks are due to Drs. Isao Tanaka and Sarin Chimnaronk (Hokkaido University) for fruitful discussion.

REFERENCES

1. Mullineux, S. T., and Lafontaine, D. L. (2012) Mapping the cleavage sites on mammalian pre-rRNAs: where do we stand? *Biochimie* **94,** 1521–1532
2. Sondalle, S. B., and Baserga, S. J. (2014) Human diseases of the SSU processome. *Biochim. Biophys. Acta* **1842,** 758–764
3. McCann, K. L., and Baserga, S. J. (2013) Mysterious ribosomopathies. *Science* **341,** 849–850
4. Piekna-Przybylska, D., Decatur, W. A., and Fournier, M. J. (2008) The 3D rRNA modification maps database: with interactive tools for ribosome analysis. *Nucleic Acids Res.* **36,** D178–D183
5. Reichow, S. L., Hamma, T., Ferré-D'Amaré, A. R., and Varani, G. (2007) The structure and function of small nucleolar ribonucleoproteins. *Nucleic Acids Res.* **35,** 1452–1464
6. Thomas, G., Gordon, J., and Rogg, H. (1978) N^4-Acetylcytidine: a previously unidentified labile component of the small subunit of eukaryotic ribosomes. *J. Biol. Chem.* **253,** 1101–1105
7. McCarroll, R., Olsen, G. J., Stahl, Y. D., Woese, C. R., and Sogin, M. L. (1983) Nucleotide sequence of the dictyostelium discoideum small-subunit ribosomal ribonucleic acid inferred from the gene sequence: evolutionary implication. *Biochemistry* **22,** 5858–5868
8. Ito, S., Akamatsu, Y., Noma, A., Kimura, S., Miyauchi, K., Ikeuchi, Y., Suzuki, T., and Suzuki, T. (2014) A single acetylation of 18 S rRNA is essential for biogenesis of the small ribosomal subunit in *Saccharomyces cerevisiae*. *J. Biol. Chem.* **289,** 26201–26212
9. Suzuki, T., Ikeuchi, Y., Noma, A., Suzuki, T., and Sakaguchi, Y. (2007) Mass spectrometric identification and characterization of RNA-modifying enzymes. *Methods Enzymol.* **425,** 211–229
10. Miyauchi, K., Kimura, S., and Suzuki, T. (2013) A cyclic form of N^6-threonylcarbamoyladenosine as a widely distributed tRNA hypermodification. *Nat. Chem. Biol.* **9,** 105–111
11. Katoh, T., and Suzuki, T. (2007) Specific residues at every third position of siRNA shape its efficient RNAi activity. *Nucleic Acids Res.* **35,** e27
12. Chi, Y. H., Haller, K., Peloponese, J. M., Jr., and Jeang, K. T. (2007) Histone acetyltransferase hALP and nuclear membrane protein hsSUN1 function in de-condensation of mitotic chromosomes. *J. Biol. Chem.* **282,** 27447–27458
13. Sampson, J. R., and Uhlenbeck, O. C. (1988) Biochemical and physical characterization of an unmodified yeast phenylalanine transfer RNA transcribed *in vitro*. *Proc. Natl. Acad. Sci. U.S.A.* **85,** 1033–1037
14. Machnicka, M. A., Milanowska, K., Osman Oglou, O., Purta, E., Kurkowska, M., Olchowik, A., Januszewski, W., Kalinowski, S., Dunin-Horkawicz, S., Rother, K. M., Helm, M., Bujnicki, J. M., and Grosjean, H. (2013) MODOMICS: a database of RNA modification pathways–2013 update. *Nucleic Acids Res.* **41,** D262–D267
15. Ikeuchi, Y., Kitahara, K., and Suzuki, T. (2008) The RNA acetyltransferase driven by ATP hydrolysis synthesizes N^4-acetylcytidine of tRNA anticodon. *EMBO J.* **27,** 2194–2203
16. Chimnaronk, S., Suzuki, T., Manita, T., Ikeuchi, Y., Yao, M., Suzuki, T., and Tanaka, I. (2009) RNA helicase module in an acetyltransferase that modifies a specific tRNA anticodon. *EMBO J.* **28,** 1362–1373
17. Lv, J., Liu, H., Wang, Q., Tang, Z., Hou, L., and Zhang, B. (2003) Molecular cloning of a novel human gene encoding histone acetyltransferase-like protein involved in transcriptional activation of hTERT. *Biochem. Biophys. Res. Commun.* **311,** 506–513
18. Kong, R., Zhang, L., Hu, L., Peng, Q., Han, W., Du, X., and Ke, Y. (2011) hALP, a novel transcriptional U three protein (t-UTP), activates RNA polymerase I transcription by binding and acetylating the upstream binding factor (UBF). *J. Biol. Chem.* **286,** 7139–7148
19. Shen, Q., Zheng, X., McNutt, M. A., Guang, L., Sun, Y., Wang, J., Gong, Y., Hou, L., and Zhang, B. (2009) NAT10, a nucleolar protein, localizes to the midbody and regulates cytokinesis and acetylation of microtubules. *Exp. Cell Res.* **315,** 1653–1667
20. Larrieu, D., Britton, S., Demir, M., Rodriguez, R., and Jackson, S. P. (2014) Chemical inhibition of NAT10 corrects defects of laminopathic cells. *Science* **344,** 527–532
21. Zhang, H., Hou, W., Wang, H. L., Liu, H. J., Jia, X. Y., Zheng, X. Z., Zou, Y. X., Li, X., Hou, L., McNutt, M. A., and Zhang, B. (2014) GSK-3β-regulated *N*-acetyltransferase 10 is involved in colorectal cancer invasion. *Clin. Cancer Res.* **20,** 4717–4729
22. Tan, T. Z., Miow, Q. H., Huang, R. Y., Wong, M. K., Ye, J., Lau, J. A., Wu, M. C., Bin Abdul Hadi, L. H., Soong, R., Choolani, M., Davidson, B., Nesland, J. M., Wang, L. Z., Matsumura, N., Mandai, M., Konishi, I., Goh, B. C., Chang, J. T., Thiery, J. P., and Mori, S. (2013) Functional genomics identifies five distinct molecular subtypes with clinical relevance and pathways for growth control in epithelial ovarian cancer. *EMBO Mol Med.* **5,** 1051–1066
23. He, C. (2010) Grand challenge commentary: RNA epigenetics? *Nat. Chem. Biol.* **6,** 863–865
24. McLuckey, S. A., Van Berkel, G. J., and Glish, G. L. (1992) Tandem mass-spectrometry of small, multiply charged oligonucleotides. *J. Am. Soc. Mass Spectrom.* **3,** 60–70